
Article:
Saiz-Lomas, J., Petri, M. orcid.org/0000-0002-3740-6106, Lee, I. Y. et al. (28 more authors) (2023) The spectroscopic quadrupole moment of the 21+ state of 12C:A benchmark of theoretical models. Physics Letters B. 138114. ISSN 0370-2693

https://doi.org/10.1016/j.physletb.2023.138114

Physics Letters B 845 (2023) 138114

Contents lists available at ScienceDirect

Physics Letters B

journal homepage: www.elsevier.com/locate/physletb

The spectroscopic quadrupole moment of the 2_1^+ state of ^{12}C: A benchmark of theoretical models

J. Saiz-Lomas [a], M. Petri [a,*], I.Y. Lee [b], I. Syndikus [c], S. Heil [c], J.M. Allmond [e], L.P. Gaffney [d], J. Pakarinen [f], H. Badran [f], T. Calverley [d,f], D.M. Cox [f], U. Forsberg [a,f], T. Grahn [f], P. Greenlees [f], K. Hadyńska-Klęk [g,1], J. Hilton [d,f], M. Jenkinson [a], R. Julin [f], J. Konki [f], A.O. Macchiavelli [b,2], M. Mathy [c], J. Ojala [f], P. Papadakis [f,3], J. Partanen [f], P. Rahkila [f], P. Ruotsalainen [f], M. Sandzelius [f], J. Sarén [f], S. Stolze [f], J. Uusitalo [f], R. Wadsworth [a]

[a] School of Physics, Engineering and Technology, University of York, York, United Kingdom
[b] Nuclear Science Division, Lawrence Berkeley National Laboratory, Berkeley, CA, USA
[c] Institut für Kernphysik, Technische Universität Darmstadt, Darmstadt, Germany
[d] Department of Physics, University of Liverpool, Liverpool, UK
[e] Physics Division, Oak Ridge National Laboratory, Oak Ridge, TN, USA
[f] Department of Physics, University of Jyväskylä, P.O. Box 35, FI-40014 Jyväskylä, Finland
[g] Department of Physics, University of Surrey, Guildford, United Kingdom

ARTICLE INFO

Article history:
Received 24 August 2022
Received in revised form 17 May 2023
Accepted 31 July 2023
Available online 8 August 2023
Editor: B. Blank

ABSTRACT

The spectroscopic quadrupole moment of the first 2^+ state of ^{12}C has been measured employing the Coulomb-excitation re-orientation technique. Our result of $Q_s(2_1^+) = +9.3^{+3.5}_{-3.8}$ efm^2 suggests a larger oblate deformation than previously reported. Combining this with the consistently re-analyzed adopted value, we present the most precise value to date of $Q_s(2_1^+) = +9.5(18)$ efm^2, which is consistent with a geometrical rotor description. This simple outcome is compared to state-of-the-art shell-model, mean-field, ab initio calculations, cluster-based and geometrical-like theories, which show varying degrees of emergent quadrupole collectivity.

1. Introduction

In the quest to understand the structure of the atomic nucleus and its many facets, experimental benchmarks of key spectroscopic information provide unparalleled opportunities to test modern nuclear theories and advance our understanding of nuclear structure. Despite the many experimental efforts devoted to probe exotic nuclei and observe modifications of their structure (see, e.g., [1]), stable nuclei still provide valuable benchmarks to further our knowledge of atomic nuclei. The particular case of ^{12}C is of great interest because of the implications that its structure, specifically the Hoyle state, has on astrophysics and the creation of carbon-based life on earth. At the same time, ^{12}C is, interestingly, one of the very few nuclei with oblate deformation in the ground state [2,3]. The interplay between cluster- and shell-model-like features in ^{12}C [4] still challenges nuclear theory and places this nucleus at the forefront of modern experimental and theoretical investigations.

Electromagnetic diagonal matrix elements, accessed for example through the spectroscopic quadrupole moment, are very sensitive to nuclear deformation, to the coupling of proton and neutron degrees of freedom, to clustering, and to subtle components of the nuclear wave function. Indeed, the first 2^+ state of ^{12}C, 2_1^+, at 4.44 MeV and its spectroscopic quadrupole moment, $Q_s(2_1^+)$, offers a sensitive probe to test many nuclear theories, from shell model and mean-field approaches [3,5–8], to ab initio calculations [9–12], to cluster-based and geometrical-like theories [4,13–17].

In this Letter we report on the measurement of the spectroscopic quadrupole moment $Q_s(2_1^+)$ of ^{12}C, employing the Coulomb-excitation re-orientation technique. The result is consistent with previous measurements [18,19]. When we re-analyze the experiment of [18] using consistent values for the transition strength and nuclear polarizability constant (more details in Sec-

* Corresponding author.
E-mail address: marina.petri@york.ac.uk (M. Petri).
[1] Present address: Heavy Ion Laboratory, University of Warsaw, Poland.
[2] Present address: Physics Division, Oak Ridge National Laboratory, Oak Ridge, Tennessee, USA.
[3] Present address: STFC Daresbury Laboratory, Daresbury, Warrington, WA4 4AD, UK.

https://doi.org/10.1016/j.physletb.2023.138114

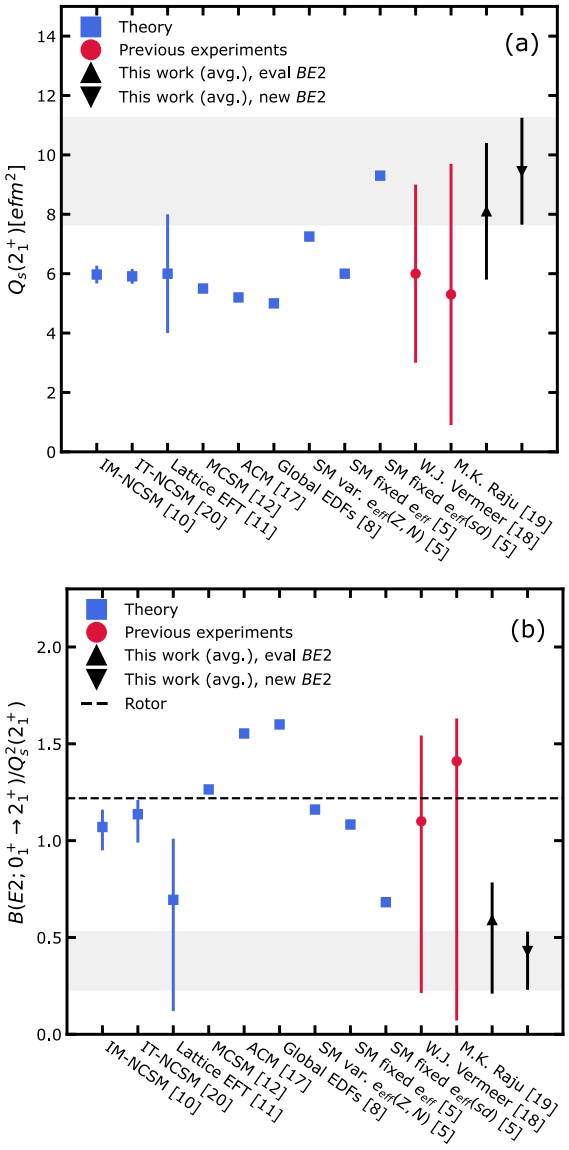

Fig. 1. Representative theoretical (blue filled squares) and literature experimental values (red filled circles) for the (a) $Q_s(2_1^+)$ and (b) dimensionless ratio $B(E2;0_1^+ \rightarrow 2_1^+)/Q_s^2(2_1^+)$ of ^{12}C, and how they compare with the value extracted from this work (black filled triangles). From the left to the right: In Medium - No Core Shell Model (IM-NCSM) and Importance Truncated - No Core Shell Model (IT-NCSM) using 2- (NN) and 3-body (3N) (NN+3N) chiral Effective-Field-Theory (EFT) interactions [10,20], lattice EFT at Leading Order (LO) [11], no-core ab initio Monte Carlo Shell Model (MCSM) using the Daejeon16 interaction [12], Algebraic Cluster Model [17], global Energy Density Functionals [8], Shell-Model calculations using variable and fixed effective charges (e_{eff}) [5], previous experimental values measured by Vermeer *et al.* [18] and by Raju et al. [19]. The experimental values from this work (black filled triangles) are obtained using $\kappa = 1.44(3)$ (see text for details) and $B(E2;0_1^+ \rightarrow 2_1^+) = 39.7(20)e^2fm^4$ [21] (eval BE2) and $B(E2;0_1^+ \rightarrow 2_1^+) = 38.15(95)e^2fm^4$ [20] (new BE2). The experimental result we present in this plot is the result from the present experiment when averaged with a consistently re-analyzed value from Vermeer *et al.* [18] (This work (avg.)). In (b) we also indicate the symmetric rotor limit. A single $p_{1/2} \otimes p_{3/2}^{-1}$ particle-hole excitation will give a ratio of 4.

tion 2) and combine this with our result, we present a significant improvement over the previous measurements, see Fig. 1. In this work we average our result with the one from [18] since both experiments have similar experimental sensitivity to the reorientation effect (40% for the current experiment and 20% for [18]), and a 50% uncertainty for the $Q_s(2_1^+)$, while the measurement of [19] has a 10% sensitivity and a 100% uncertainty since it probed forward scattering angles. Our result challenges nuclear theory by revealing some tension between their predictions and the experimental data. Interestingly, the experimental observables suggest that ^{12}C can be considered as either a triangular structure or an oblate spheroid. In both scenarios, superfluidity appears to play a decisive role.

2. Experimental details and results

The experiment was performed at the JYFL accelerator laboratory at the University of Jyväskylä, Finland. A 47.65 MeV $^{12}C^{4+}$ ion beam delivered by the K130 cyclotron bombarded a 300 μg/cm^2 thick ^{208}Pb target (99.0% enriched) on a 40 μg/cm^2 ^{12}C backing, Coulomb exciting both the projectile and the target. The centroid of the beam energy distribution was measured to be 47.65 MeV with a 0.1% uncertainty; the beam energy spread was $\Delta E/E = 1\%$ (FWHM).

The subsequent de-exciting γ rays following the population of the 2_1^+ state at 4439 keV in ^{12}C, and 3_1^- and 2_1^+ states at 2614 keV and 4085 keV in ^{208}Pb, respectively, were measured by the 15 Compton-suppressed Eurogam Phase-I and 24 Clover Ge detectors in add-back mode of the JUROGAM II array [22]. A double-sided silicon CD-type detector (Micron S2), consisting of 16 sectors and 48 rings, was used to detect backward-scattered ^{12}C particles in coincidence. The detector was placed at 57.9 mm from the target subtending polar angles between 149.0° and 158.6° with respect to the beam direction.

The energy and relative efficiency calibration for the JUROGAM II array was performed with a ^{66}Ga source. Emission probabilities for eighteen strong lines, from 834 keV to 4806 keV, are known to better than 1% in ^{66}Ga [23]. The γ-ray emissions at 2752 keV and 4461 keV in ^{66}Ga, close to the 2614 keV and 4439 keV in ^{208}Pb and ^{12}C respectively, made this radioactive source an ideal candidate to minimize the systematic uncertainties in the relative efficiency of the array. The radioactive source was produced at JYFL in situ using a 11 MeV proton beam on a natural zinc target through the ^{66}Zn(p,n)^{66}Ga and ^{67}Zn(p,2n)^{66}Ga reaction channels.

The particle detector was calibrated using a triple α source containing ^{239}Pu, ^{241}Am and ^{244}Cm, which emits alpha particles at three distinct energies between 5 and 6 MeV. The elastically scattered ^{12}C particles at each scattering angle θ, where θ is determined by each ring in the silicon detector, were used as higher-energy calibration points.

A particle-γ coincidence window of 90 ns was set and the corresponding γ-ray spectra were further cleaned by subtracting random coincidence events outside this time window. Additionally, only single hit events in the particle detector were considered, i.e., events where only one hit in one of the rings and one of the sectors were recorded. Finally, particle-energy gates on the inelastic peaks corresponding to the observed γ-ray transitions, i.e., excitation of the 2_1^+ state in ^{12}C and the first 3_1^- and 2_1^+ states in ^{208}Pb, were applied.

Doppler correction of the γ-ray energies was performed using the angle between the Ge detector and the velocity vector of the emitting nucleus (^{12}C or ^{208}Pb) calculated from the angle of the detected ^{12}C in the segment of the Si detector. Fig. 2 shows the background-subtracted and Doppler-corrected γ-ray energy spectra generated with particle coincidence, time, and inelastic particle-energy gates for the 2_1^+ excitation in ^{12}C. Similar spectra with Doppler correction for the target excitation and the corresponding inelastic particle-energy gates for the 3_1^- and 2_1^+ excitations in ^{208}Pb are included in Fig. 3. The measured γ-ray yields for the different transitions in ^{12}C and ^{208}Pb were found to be $N_\gamma^P(2_1^+) = 2023(255)$, $N_\gamma^T(3_1^-) = 97962(401)$ and $N_\gamma^T(2_1^+) = 2115(252)$, respectively.

In order to ensure pure electromagnetic interaction between the projectile and the target, the distance between the nuclear

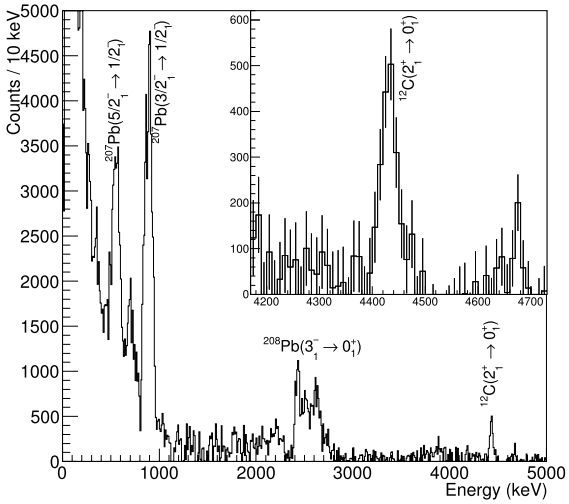

Fig. 2. Background subtracted and Doppler-corrected γ-ray energy spectrum generated with particle coincidence, time, and inelastic particle-energy gates for the 2^+_1 excitation in ^{12}C. The inset focuses on the γ ray of interest.

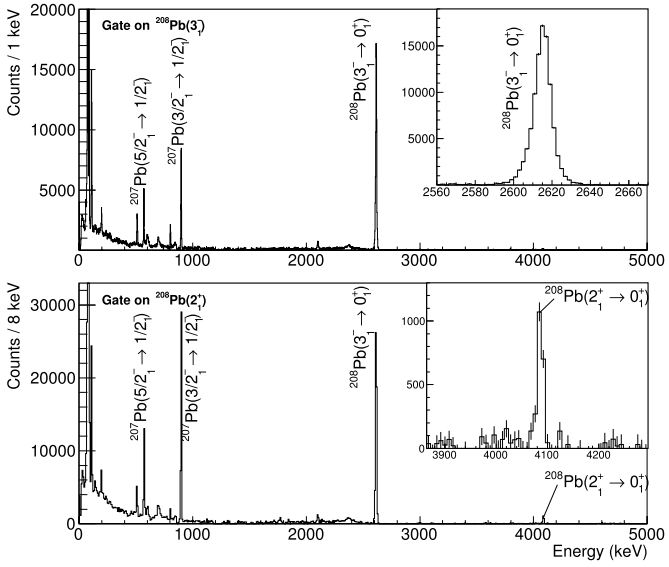

Fig. 3. Background subtracted and Doppler-corrected γ-ray energy spectrum with particle coincidence, time, and inelastic particle-energy gates for the 3^-_1 (top) and 2^+_1 (bottom) excitation in ^{208}Pb. The insets focus on the γ rays of interest.

surfaces must be large enough to avoid the effect of Coulomb-nuclear interference in the cross-section. In the present experiment, the minimum separation distance between nuclear surfaces was $s \approx 5.6$ fm, informed by experimental data on light nuclei [24] and in conformity with the 5 fm of Cline's prescription [25]. In addition, the authors in [26] performed a systematic study of the Coulomb-excitation probability as a function of the beam energy for the ^{12}C+^{208}Pb system for beam energies ranging from 52 to 58 MeV at a scattering angle of $\theta_{\rm LAB} = 90°$. In their published work it was concluded that Coulomb-nuclear interference effects started to arise at 58 MeV ($s = 5.1$ fm) and were therefore not present in their measurement at 56 MeV ($s = 5.6$ fm) for the ^{12}C+^{208}Pb system. This further supports the absence of Coulomb-nuclear interference effects in our experiment.

In addition to re-orientation, virtual electric-dipole excitations via the Giant Dipole Resonance (GDR) also contribute to second-order to the population of the 2^+_1 state, especially for the case of light nuclei. In this sense, the 2^+_1 state in ^{12}C may be populated through a two-step process of the type $0^+_1 \rightarrow 1^-_{GDR} \rightarrow 2^+_1$. The probability of the 2^+_1 state being excited through the GDR can be expressed in terms of the (-2) moment of the total photo-absorption cross-section (σ_{-2}). The σ_{-2} value can be estimated by the hydrodynamic model for heavier nuclei, however, for light nuclei one relies on experimental information, which is very scarce. The deviation of σ_{-2} from the hydrodynamic model is typically expressed in terms of the polarizability constant κ [27]

$$\sigma_{-2} = 3.5\kappa A^{5/3}\ \mu\text{b/MeV}. \tag{1}$$

The most featured compilation of photo-neutron cross-section data was evaluated by Dietrich and Berman in 1988 [28], which came recently under question [29]. For ^{12}C there are several experiments providing different results for σ_{-2}. Out of these, the experimental work of [30] measured with high precision the total photo-absorption cross-section for ^{12}C and yielded a value of the nuclear polarizability constant of $\kappa = 1.44(3)$ ($\sigma_{-2} = 316(5)$ μb/MeV). This value of κ is in excellent agreement with $\kappa = 1.5(1)$ obtained by recent NCSM calculations using the chiral NN+3NF350 interaction [19]; the latter is reported in [19] as $\kappa = 2.2(2)$ using the formula $\sigma_{-2} = 2.38\kappa A^{5/3}$ μb/MeV from [31], which is the equivalent of $\kappa = 1.5(1)$ using Eq. (1). Therefore, in the present analysis we use $\kappa = 1.44(3)$. We will also present the value of $Q_s(2^+_1)$ as a function of σ_{-2} (or κ).

The diagonal quadrupole matrix element of the 2^+_1 state in ^{12}C was extracted using the semi-classical coupled-channel Coulomb-excitation least-squares code GOSIA2 [32]. The code handles the simultaneous analysis of both target and projectile excitations by minimizing the χ^2 function in parallel for both collision partners [33]. In the present analysis, the normalisation transition was chosen to be the well-known $B(E3; 0^+_1 \rightarrow 3^-_1) = 0.611(9)\,\text{e}^2\text{b}^3$ [21] of the ^{208}Pb target. In this way, the code uses these known literature data to convert the measured ^{12}C 2^+_1 γ-ray yield to an absolute excitation cross section. The GOSIA2 input includes additional relevant spectroscopic information such as lifetimes, branching ratios, matrix elements and nuclear polarizability, and also experimental information such as the particle-detector geometry, γ-ray detector geometry and relative efficiency, target thickness and beam energy. Using the analysis method described in [33], a 2-dimensional χ^2 surface in the plane of the transitional $\langle 2^+_1||E2||0^+_1\rangle$ and diagonal $\langle 2^+_1||E2||2^+_1\rangle$ matrix elements, $\langle 2^+_1||E2||0^+_1\rangle$-$\langle 2^+_1||E2||2^+_1\rangle$ plane, can be constructed to describe the excitation process in the projectile. The global minimum of the surface, $\chi^2_{\rm min}$, will correspond to the set of matrix elements that best reproduces the measured experimental yields. The 1σ uncertainty contour defined by $\chi^2 < \chi^2_{\rm min} + 1$ will provide the correlated uncertainty between the parameters. Fig. 4 shows the 1σ contour of the two-dimensional χ^2 surface using the literature value of the $B(E2; 0^+_1 \rightarrow 2^+_1) = 39.7(20)$ e^{2}fm^4 [21] (also written as $B(E2)$ hereafter) and the default value of the nuclear polarizability constant $\kappa = 1$. The projected 1σ uncertainties yield a value of the diagonal matrix element of $\langle 2^+_1||E2||2^+_1\rangle = 8.8^{+4.1}_{-4.5}$ efm^2, which corresponds to a value of the spectroscopic quadrupole moment of $Q_s(2^+_1) = +6.7^{+3.5}_{-3.8}$ efm^2, $Q_s(2^+_1) = 0.75793\,\langle 2^+_1||E2||2^+_1\rangle$. This result includes an additional ± 0.35 efm^2 arising from the 0.1% uncertainty in the beam energy centroid.

The uncertainty in the $Q_s(2^+_1)$ includes the error in all γ-ray yields and all propagated uncertainties from the spectroscopic data included in the χ^2 minimisation. This method accounts for all correlated and uncorrelated uncertainties in the fitting of the matrix elements in the projectile and in the target. The uncertainty arising from the effect of higher-lying states in both collision partners, the accuracy of the semi-classical description, the nuclear de-orientation, mutual projectile and target excitation, detector ge-

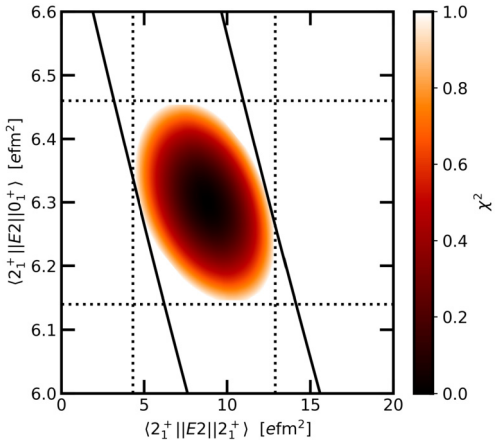

Fig. 4. Two-dimensional total $\chi^2 < \chi^2_{\rm min}+1$ surface obtained with GOSIA2 with respect to the diagonal $\langle 2_1^+||E2||2_1^+\rangle$ and transitional $\langle 2_1^+||E2||0_1^+\rangle$ matrix elements in ^{12}C. The solid lines correspond to the 1σ contours of the Coulomb-excitation. The horizontal dashed lines correspond to the 1σ uncertainty of $\langle 2_1^+||E2||0_1^+\rangle = 6.30(16)$ efm^2. The vertical dashed lines indicate the projected 1σ uncertainties of the resulting diagonal matrix element $\langle 2_1^+||E2||2_1^+\rangle = 8.8^{+4.1}_{-4.5}$ efm^2. This analysis uses the default value of the nuclear polarizability constant $\kappa = 1$.

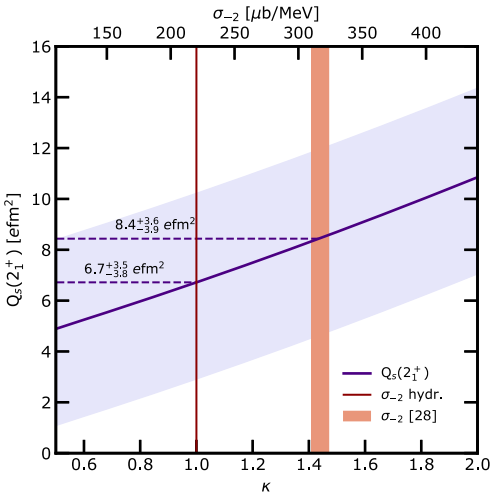

Fig. 5. Extracted $Q_s(2_1^+)$ (dark violet line) from the GOSIA2 fit to the experimental γ-ray yields as a function of the nuclear polarizability constant κ (total photoabsorption cross-section σ_{-2}) using the evaluated value of $B(E2)$ [21]. The uncertainties on the final result are represented as the shaded violet area in the figure. The values of the nuclear polarizability constant $\kappa = 1$ and $\kappa = 1.44(3)$ are also indicated.

ometry and target thickness were investigated and found to have a negligible effect in the final result.

The contribution of the nuclear polarizability will not change the size of the 1σ contours of Fig. 4 and, since its effect is systematic, it will only shift the position of the $\chi^2_{\rm min}$ in the $\langle 2_1^+||E2||0_1^+\rangle$-$\langle 2_1^+||E2||2_1^+\rangle$ plane. The uncertainty in the polarizability constant κ can be propagated in quadrature. Fig. 5 shows the extracted $Q_s(2_1^+)$ from the GOSIA2 fit to the experimental γ-ray yields as a function of the nuclear polarizability constant κ using the adopted value of $B(E2)$ [21]. For $\kappa = 1.44(3)$ our analysis yields a value of $Q_s(2_1^+) = +8.4^{+3.6}_{-3.9}$ efm^2, which accounts for an additional ± 0.1 efm^2 from the uncertainty in κ. The same analysis using the most recent value of $B(E2; 0_1^+ \rightarrow 2_1^+) = 38.15(95)$e^{2}fm^4 [20] yields $Q_s(2_1^+) = +9.3^{+3.5}_{-3.8}$ efm^2 for $\kappa = 1.44(3)$, see Table 1.

The result of [18] can be re-analysed using the most up-to-date values of $B(E2)$ and κ, and can be combined with the present work to further constrain the experimental uncertainties in

Table 1
Obtained result for the $Q_s(2_1^+)$ of ^{12}C from the present work and re-analyzing the data from [18] for nuclear polarizability of $\kappa = 1.44(3)$, and $B(E2) = 39.7(20)$ [21] and 38.15(95) e^{2}fm^4 [20]. The weighted average for each $B(E2)$ value is also listed, $Q_s(2_1^+)^{wa}$.

$Q_s(2_1^+)$ [efm^2]	$B(E2)$	Data	$Q_s(2_1^+)^{wa}$ [efm^2]
$+8.4^{+3.6}_{-3.9}$	[21]	this work	$+8.1 \pm 2.3$
$+7.8 \pm 3.0$	[21]	re-analyzed [18]	
$+9.3^{+3.5}_{-3.8}$	[20]	this work	$+9.5 \pm 1.8$
$+9.5 \pm 2.0$	[20]	re-analyzed [18]	

$Q_s(2_1^+)$. Table 1 includes the data from [18] and this work assuming $\kappa = 1$ and 1.44(3), and $B(E2) = 39.7(20)$ and 38.15(95) e^{2}fm^4 [20]. There is an excellent agreement between both experiments.

For $\kappa = 1.44(3)$, the weighted average of both experiments yields $Q_s(2_1^+) = +8.1(23)$ efm^2 for the evaluated value of the $B(E2)$ [21] and $Q_s(2_1^+) = +9.5(18)$ efm^2 for the most recent measurement for the $B(E2)$ [20]. These values can for the first time discriminate between different nuclear theories. We will use $Q_s(2_1^+) = +9.5(18)$ efm^2 and refer to as "our result" from hereafter.

In the rotational model this gives an intrinsic quadrupole moment of $Q_o(2_1^+) = -(7/2)\,Q_s(2_1^+) = 33(6)$ efm^2, corresponding to an oblate shape [34].

3. Discussion

To start our discussion we mention that the present results as well as other structural observables of ^{12}C could be readily understood in terms of a rigid asymmetric top [35,36], a first indication of which is given by the fact that the experimental energy ratio $E(4_2^+)/E(2_1^+) = 3.17$ is consistent with axial asymmetry[4]; the experimental 4_1^+ level is associated with the Hoyle state [37]. In this geometric description, the shape of ^{12}C can be described by either a spheroid with the usual β and γ quadrupole shape parameters or three (point) alpha (α) particles forming an isosceles triangle with an opening angle of Ω. The ratio $B(E2; 0_1^+ \rightarrow 2_1^+)/Q_s^2(2_1^+)$ can only be described using irrotational flow like (relative) moments of inertia and it is relatively constant over a range of axial asymmetries, namely $\Omega \approx 50^\circ - 70^\circ$ and $\gamma \approx 40^\circ - 80^\circ$; the data cannot distinguish between the spheroidal and the triangular description. When considering the overall absolute scale, the moments of inertia required to reproduce the energy of the 2_1^+ is $\approx 60\%$ of the rigid moment of inertia. An interesting picture thus emerges in which the structure of ^{12}C could be considered as an example of a supersolid [38].

We now proceed to compare in Fig. 1 our result for $Q_s(2_1^+)$ of ^{12}C with various theoretical predictions. Although the high energy of the γ-ray transition (4.44 MeV) and the low Coulomb excitation cross section make this a challenging measurement, it is evident that our result places an important constraint to the theory.

It is interesting that the ab initio calculations [10,20,11,12] firmly predict $Q_s(2_1^+) \approx +6$ efm^2. This lies at the very edge (within 2σ) of the experimental value. Similarly, results from the Algebraic Cluster Model [17] and the global EDFs [8] lie within 3σ of the experimental value. The shell-model results have a strong dependence on the effective charges [5] used. Specifically, we note that when using isospin-dependent effective charges (see [6]), the spectroscopic quadrupole moment agrees well with experiment with similar predictions either using the WBP interaction [39] or a monopole-based universal interaction [5]. A combination of the latter with the conventional effective charges for the *sd* shell,

[4] A symmetric top should yield $E(4^+)/E(2^+) = 3.33$.

$e_p = 1.3$ and $e_n = 0.5$, pushes the prediction of the spectroscopic quadrupole moment towards the higher end of the present measurement (SM fixed $e_{eff}(sd)$ in Fig. 1(a)).

When trying to benchmark theoretical predictions with our experimental result, it is important to consider also the calculated $B(E2)$ transition strength, and the dimensionless ratio $B(E2)/Q_s^2$, which offers an appealing indicator to extract structural information on even-even nuclei [40]. In particular to our discussion, this ratio is important to assess any convergence limitations that the ab initio calculations face given the sensitivity of the $E2$ operator to the long-range behaviour (tails) of the wavefunctions involved. In fact, several studies [10,41,42] have shown the robustness of this ratio, that converges faster than the two observables individually. An inspection of Fig. 1(b), comparing our experimental value to the theoretical results,[5] could suggest that the microscopic interactions need to be revisited, if, to some extent, the ratio minimizes the convergence issues. As for the effective interaction shell model, where the truncation effects are embedded in the effective charges, one should pay attention to the comparisons in Figs. 1(a) and 1(b). Although the SM fixed $e_{eff}(sd)$ of [5] appears to explain (partly) the data, the use of sd charges for ^{12}C may be questionable.

As a final remark, there are still clear challenges faced by the shell model and ab initio methods in capturing the full geometry of an asymmetric top in their large, but still limited Hilbert space.

4. Summary

With this work we have presented the most precise to date value for the spectroscopic quadrupole moment of the 2_1^+ state of ^{12}C. Our result suggests a larger oblate deformation than previously thought for this state and motivates further theoretical investigations. It is anticipated that future experimental works [43], informed by the present work, will shed further light on the structure of ^{12}C.

Declaration of competing interest

The authors declare that they have no known competing financial interests or personal relationships that could have appeared to influence the work reported in this paper.

Data availability

Data will be made available on request.

Acknowledgements

The authors acknowledge C. Bertulani, A. Vitturi, A. Moro, M. Gomez, J. M. Quesada, M. Zielinska, and C. Barton for enlightening discussions, and I. Moore for proposing and supporting the production of the ^{66}Ga source. This work was supported by the Deutsche Forschungsgemeinschaft (DFG, German Research Foundation) – Projektnummer 279384907 – SFB 1245, the Royal Society under contract number UF150476, the UK STFC under grant numbers ST/L005727/1, ST/P003885/1, the UK STFC ERF fellowship ST/R004056/1, and by the Director, Office of Science, Office of Nuclear Physics, of the U.S. Department of Energy under Contract No. DE-AC02-05CH11231 (LBNL). This project has received funding from the EU HORIZON2020 programme "Infrastructures", project number 654002 (ENSAR2). U. Forsberg would like to thank Birgit and Hellmuth Hertz' Foundation for financial support.

[5] The error bars in Fig. 1(b) have been calculated by using a Monte Carlo method starting with Gaussian distributions of the matrix elements to produce the probability distribution of the ratio $B(E2)/Q_s^2$. This distribution is asymmetric, and we present the results using the ratio of the experimental values as the centre point and the 68% confidence range of the distribution as the error bars. The same method is used to calculate the ratio of our work when averaged with Vermeer's result (This work (avg.)), as well as theoretical results with known uncertainties.

References

[1] T. Otsuka, A. Gade, O. Sorlin, T. Suzuki, Y. Utsuno, Evolution of shell structure in exotic nuclei, Rev. Mod. Phys. 92 (2020) 015002, https://doi.org/10.1103/RevModPhys.92.015002.
[2] I. Hamamoto, B.R. Mottelson, Further examination of prolate-shape dominance in nuclear deformation, Phys. Rev. C 79 (2009) 034317, https://doi.org/10.1103/PhysRevC.79.034317.
[3] I. Hamamoto, Oblate deformation of light neutron-rich even-even nuclei, Phys. Rev. C 89 (2014) 057301, https://doi.org/10.1103/PhysRevC.89.057301.
[4] Y. Kanada-En'yo, The structure of ground and excited states of ^{12}C, Prog. Theor. Phys. 117 (4) (2007) 655–680, https://doi.org/10.1143/PTP.117.655, https://academic.oup.com/ptp/article-pdf/117/4/655/5152706/117-4-655.pdf.
[5] C. Yuan, T. Suzuki, T. Otsuka, F. Xu, N. Tsunoda, Shell-model study of boron, carbon, nitrogen, and oxygen isotopes with a monopole-based universal interaction, Phys. Rev. C 85 (2012) 064324, https://doi.org/10.1103/PhysRevC.85.064324.
[6] H. Sagawa, X.R. Zhou, X.Z. Zhang, T. Suzuki, Deformations and electromagnetic moments in carbon and neon isotopes, Phys. Rev. C 70 (2004) 054316, https://doi.org/10.1103/PhysRevC.70.054316.
[7] J.M. Yao, J. Meng, P. Ring, Z.X. Li, Z.P. Li, K. Hagino, Microscopic description of quantum shape fluctuation in C isotopes, Phys. Rev. C 84 (2011) 024306, https://doi.org/10.1103/PhysRevC.84.024306.
[8] P. Marević, J.-P. Ebran, E. Khan, T. Nikšić, D. Vretenar, Cluster structures in ^{12}C from global energy density functionals, Phys. Rev. C 99 (2019) 034317, https://doi.org/10.1103/PhysRevC.99.034317.
[9] P. Maris, J.P. Vary, A. Calci, J. Langhammer, S. Binder, R. Roth, ^{12}C properties with evolved chiral three-nucleon interactions, Phys. Rev. C 90 (2014) 014314, https://doi.org/10.1103/PhysRevC.90.014314.
[10] A. Calci, R. Roth, Sensitivities and correlations of nuclear structure observables emerging from chiral interactions, Phys. Rev. C 94 (1) (2016) 014322, https://doi.org/10.1103/PhysRevC.94.014322, arXiv:1601.07209.
[11] E. Epelbaum, H. Krebs, T.A. Lähde, D. Lee, U.-G. Meißner, Structure and rotations of the hoyle state, Phys. Rev. Lett. 109 (2012) 252501, https://doi.org/10.1103/PhysRevLett.109.252501.
[12] T. Otsuka, T. Abe, T. Yoshida, Y. Tsunoda, N. Shimizu, N. Itagaki, Y. Utsuno, J. Vary, P. Maris, H. Ueno, α-clustering in atomic nuclei from first principles with statistical learning and the Hoyle state character, Nat. Commun. 13 (1) (2022) 2234, https://doi.org/10.1038/s41467-022-29582-0.
[13] J. Casal, L. Fortunato, E.G. Lanza, A. Vitturi, Alpha-induced inelastic scattering and alpha-transfer reactions in ^{12}C and ^{16}O within the algebraic cluster model, Eur. Phys. J. A 57 (1) (2021) 33, https://doi.org/10.1140/epja/s10050-021-00347-5.
[14] T. Neff, H. Feldmeier, Cluster structures within fermionic molecular dynamics, in: Proceedings of the 8th International Conference on Clustering Aspects of Nuclear Structure and Dynamics, Nucl. Phys. A 738 (2004) 357–361, https://doi.org/10.1016/j.nuclphysa.2004.04.061, https://www.sciencedirect.com/science/article/pii/S0375947404006025.
[15] Roelof Bijker, The structure of rotational bands in alpha-cluster nuclei, EPJ Web Conf. 93 (2015) 01011, https://doi.org/10.1051/epjconf/20159301011.
[16] M. Haberichter, P.H.C. Lau, N.S. Manton, Electromagnetic transition strengths for light nuclei in the Skyrme model, Phys. Rev. C 93 (2016) 034304, https://doi.org/10.1103/PhysRevC.93.034304.
[17] R. Bijker, Symmetries and order in cluster nuclei, AIP Conf. Proc. 2150 (1) (2019) 020002, https://doi.org/10.1063/1.5124574.
[18] W. Vermeer, et al., Electric quadrupole moment of the first excited state of ^{12}C, Phys. Lett. B 122 (1) (1983) 23–26, https://doi.org/10.1016/0370-2693(83)91160-7, http://www.sciencedirect.com/science/article/pii/0370269383911607.
[19] M.K. Raju, et al., Reorientation-effect measurement of the first 2^+ state in ^{12}C: confirmation of oblate deformation, Phys. Lett. B 777 (2018) 250–254, https://doi.org/10.1016/j.physletb.2017.12.009, http://www.sciencedirect.com/science/article/pii/S0370269317309863.
[20] A. D'Alessio, T. Mongelli, M. Arnold, S. Bassauer, J. Birkhan, I. Brandherm, M. Hilcker, T. Hüther, J. Isaak, L. Jürgensen, T. Klaus, M. Mathy, P. von Neumann-Cosel, N. Pietralla, V.Y. Ponomarev, P.C. Ries, R. Roth, M. Singer, G. Steinhilber, K. Vobig, V. Werner, Precision measurement of the $E2$ transition strength to the 2_1^+ state of ^{12}C, Phys. Rev. C 102 (2020) 011302, https://doi.org/10.1103/PhysRevC.102.011302.
[21] B. Pritychenko, M. Birch, B. Singh, M. Horoi, Tables of E2 transition probabilities from the first 2^+ states in even–even nuclei, At. Data Nucl. Data Tables 107 (2016) 1–139, https://doi.org/10.1016/j.adt.2015.10.001, http://www.sciencedirect.com/science/article/pii/S0092640X15000406.
[22] J. Pakarinen, J. Ojala, P. Ruotsalainen, H. Tann, H. Badran, T. Calverley, J. Hilton, T. Grahn, P.T. Greenlees, M. Hytönen, A. Illana, A. Kauppinen, M. Luoma, P. Papadakis, J. Partanen, K. Porras, M. Puskala, P. Rahkila, K. Ranttila, J. Sarén, M.

Sandzelius, S. Szwec, J. Tuunanen, J. Uusitalo, G. Zimba, The jurogam 3 spectrometer, Eur. Phys. J. A 56 (5) (2020) 149, https://doi.org/10.1140/epja/s10050-020-00144-6.
[23] C. Baglin, et al., ^{66}Ga: a standard for high-energy calibration of ge detectors, Nucl. Instrum. Methods A 481 (1) (2002) 365–377, https://doi.org/10.1016/S0168-9002(01)01376-6, http://www.sciencedirect.com/science/article/pii/S0168900201013766.
[24] H.J. Wollersheim, Kernstruktur schnell rotierender Atomkerne, Habilitation thesis, Goethe University Frankfurt, 1992.
[25] D. Cline, Nuclear shapes studied by Coulomb excitation, Annu. Rev. Nucl. Part. Sci. 36 (1) (1986) 683–716, https://doi.org/10.1146/annurev.ns.36.120186.003343.
[26] W. Vermeer, M. Esat, J. Kuehnerand, R.H. Spear, A. Baxter, S. Hinds, Coulomb excitation of the 2.615 MeV (3^-) and 4.086 MeV (2^+) states of ^{208}Pb, Aust. J. Phys. 37 (2) (1984) 123–136.
[27] J.S. Levinger, Migdal's and Khokhlov's calculations of the nuclear photoeffect, Phys. Rev. 107 (1957) 554–558, https://doi.org/10.1103/PhysRev.107.554, https://link.aps.org/doi/10.1103/PhysRev.107.554.
[28] S.S. Dietrich, B.L. Berman, Atlas of photoneutron cross sections obtained with monoenergetic photons, At. Data Nucl. Data Tables 38 (2) (1988) 199–338, https://doi.org/10.1016/0092-640X(88)90033-2, http://www.sciencedirect.com/science/article/pii/0092640X88900332.
[29] J.N. Orce, Polarizability effects in atomic nuclei, Int. J. Mod. Phys. E 29 (03) (2020) 2030002, https://doi.org/10.1142/S0218301320300027.
[30] J. Ahrens, et al., The total absorption of photons by nuclei, Nucl. Phys. A 251 (1975) 479, https://doi.org/10.1016/0375-9474(75)90543-6.
[31] J.N. Orce, New formulas for the (-2) moment of the photoabsorption cross section, σ_{-2}, Phys. Rev. C 91 (2015) 064602, https://doi.org/10.1103/PhysRevC.91.064602.
[32] T. Czosnyka, D. Cline, C. Wu, Bull. Am. Phys. Soc. 28 (1983) 745.
[33] M. Zielinska, L. Gaffney, K. Wrzosek-Lipska, et al., Analysis methods of safe Coulomb-excitation experiments with radioactive ion beams using the GOSIA code, Eur. Phys. J. A 52 (99) (2016), https://doi.org/10.1140/epja/i2016-16099-8.
[34] A. Bohr, B. Mottelson, Nuclear Structure, Benjamin, New York, 1969.
[35] J.L. Wood, A.-M. Oros-Peusquens, R. Zaballa, J.M. Allmond, W.D. Kulp, Triaxial rotor model for nuclei with independent inertia and electric quadrupole tensors, Phys. Rev. C 70 (2004) 024308, https://doi.org/10.1103/PhysRevC.70.024308.
[36] J.M. Allmond, R. Zaballa, A.M. Oros-Peusquens, W.D. Kulp, J.L. Wood, Triaxial rotor model description of $E2$ properties in ^{186,188,190,192}Os, Phys. Rev. C 78 (2008) 014302, https://doi.org/10.1103/PhysRevC.78.014302.
[37] M. Freer, S. Almaraz-Calderon, A. Aprahamian, N.I. Ashwood, M. Barr, B. Bucher, P. Copp, M. Couder, N. Curtis, X. Fang, F. Jung, S. Lesher, W. Lu, J.D. Malcolm, A. Roberts, W.P. Tan, C. Wheldon, V.A. Ziman, Evidence for a new ^{12}C state at 13.3 mev, Phys. Rev. C 83 (2011) 034314, https://doi.org/10.1103/PhysRevC.83.034314.
[38] S. Ohkubo, J. Takahashi, Y. Yamanaka, Supersolidity of the α cluster structure in the nucleus ^{12}C, Prog. Theor. Exp. Phys. 2020 (4) (2020) 041D01, https://doi.org/10.1093/ptep/ptaa043, https://academic.oup.com/ptep/article-pdf/2020/4/041D01/33151378/ptaa043.pdf.
[39] E.K. Warburton, B.A. Brown, Effective interactions for the 0p1s0d nuclear shell-model space, Phys. Rev. C 46 (1992) 923–944, https://doi.org/10.1103/PhysRevC.46.923.
[40] Y. Sharon, N. Benczer-Koller, G. Kumbartzki, L. Zamick, R. Casten, Systematics of the ratio of electric quadrupole moments Q(2_1^+) to the square root of the reduced transition probabilities B(E2; $0_1^+ \rightarrow 2_1^+$) in even-even nuclei, Nucl. Phys. A 980 (2018) 131–142, https://doi.org/10.1016/j.nuclphysa.2018.10.027, https://www.sciencedirect.com/science/article/pii/S0375947418303002.
[41] S.L. Henderson, T. Ahn, M.A. Caprio, P.J. Fasano, A. Simon, W. Tan, P. O'Malley, J. Allen, D.W. Bardayan, D. Blankstein, B. Frentz, M.R. Hall, J.J. Kolata, A.E. McCoy, S. Moylan, C.S. Reingold, S.Y. Strauss, R.O. Torres-Isea, First measurement of the $b(e2; 3/2^- \rightarrow 1/2^-)$ transition strength in ^{7}Be: testing *ab initio* predictions for $a = 7$ nuclei, Phys. Rev. C 99 (2019) 064320, https://doi.org/10.1103/PhysRevC.99.064320, https://link.aps.org/doi/10.1103/PhysRevC.99.064320.
[42] M.A. Caprio, P.J. Fasano, P. Maris, A.E. McCoy, Quadrupole moments and proton-neutron structure in p-shell mirror nuclei, Phys. Rev. C 104 (2021) 034319, https://doi.org/10.1103/PhysRevC.104.034319, https://link.aps.org/doi/10.1103/PhysRevC.104.034319.
[43] M. Petri, I.-Y. Lee, et al., Argonne National Laboratory Experimental Proposal 1884, 2022.